THE ASTROPHYSICAL JOURNAL, 510:188–196, 1999 January 1

ON THE HADRONIC BEAM MODEL FOR GAMMA-RAY PRODUCTION IN BLAZARS

J. H. BEALL[1,2,3] AND W. BEDNAREK[4]
Received 1998 January 26; accepted 1998 August 6

ABSTRACT

We consider a model for γ-ray production in blazars in which a relativistic, highly collimated electron-proton beam interacts with a dense, compact cloud as the jet propagates through the broad- and perhaps narrow-line regions of active galactic nuclei. During the propagation of the beam through the cloud, the process of excitation of plasma waves becomes an important energy-loss mechanism, especially for mildly relativistic proton beams. We compute the expected spectra of γ-rays from the decay of neutral pions produced in hadronic collisions of the beam with the cloud, taking into account collisionless losses of the electron-proton beam. This model may explain the X-ray and TeV γ-ray (both low and high emission states) of Mrk 421 as a result of synchrotron emission of secondary pairs from the decay of charged pions and γ-ray emission from the decay of neutral pions for the plausible cloud parameters. However, clouds cannot be too hot and too dense. Otherwise, the TeV γ-rays can be attenuated by the bremsstrahlung radiation in the cloud and the secondary pairs are not able to efficiently produce synchrotron flares because of the dominant role of inverse Compton scattering. The nonvariable γ-ray emission observed from Mrk 421 in the EGRET energy range cannot be described by the γ-rays from decay of neutral pions provided that the spectrum of protons in the beam is well described by a simple power law. These γ-rays might only be produced by secondary pairs scattering the soft nonvariable X-rays, which might originate in the inner part of the accretion disk.

Subject headings: BL Lacertae objects: individual (Markarian 421) — galaxies: active — galaxies: jets — gamma rays: theory — radiation mechanisms: nonthermal

1. INTRODUCTION

Many blazar-type active galaxies have recently been detected in MeV–GeV γ-rays by detectors on board the *Compton Gamma-Ray Observatory* (*CGRO*) (von Montigny et al. 1995). Mrk 421, Mrk 501, and 1E 2344 are observed in the TeV γ-rays (Punch et al. 1992; Quinn et al. 1996; Catanese et al. 1998). The γ-ray emission of blazars is highly variable on different timescales (from months and weeks up to a fraction of an hour; e.g., Gaidos et al. 1996; Mattox et al. 1997). The spectra of flat-spectrum radio quasar blazars are well described by a power law with a spectral break from the lower energy part observed in a few sources (McNaron-Brawn et al. 1995; Schönfelder et al. 1996) and possibly a cutoff at higher energies (Pohl et al. 1997). The spectra of two BL Lac objects, Mrk 421 and Mrk 501, extend up to at least ~ 10 TeV (Krennrich et al. 1997; Aharonian et al. 1997). There is also weak evidence of emission of ~ 50 TeV photons from some nearby BL Lac objects (Mayer & Westerhoff 1996).

These observations are usually interpreted in terms of inverse Compton scattering models. These models have been discussed previously in many different geometrical scenarios (see, for example, reviews by Dermer & Schlickeiser 1992; Sikora 1994; Dermer & Gehrels 1995; Schlickeiser 1996; Bednarek 1998). Henri, Pelletier, & Roland (1993) have suggest that γ-ray emission can be produced by inverse Compton scattering of relativistically moving $e^{\pm}$ beams with the ambient radiation in the cores of BL Lac objects. Interestingly, Henri et al. also suggest that a component of these sources must be an electron-proton jet that contains most of the kinetic luminosity of the source, a supposition originally put forth by Burbidge (1956). The existence of such beams also seems to be suggested by population studies that show a significant correlation between the Doppler-corrected X-ray luminosities and X-ray variability timescales in BL Lac sources (Xie, Liu, & Wang 1995).

The γ-rays observed in blazars can also be produced in collisions of very high energy hadrons with soft radiation (e.g., Sikora et al. 1987). This mechanism is discussed in the context of γ-ray production in blazars by, e.g., Mannheim & Biermann (1992), Coppi, Kartje, & Königl (1993), Protheroe (1998), and Bednarek & Protheroe (1997a, 1997b).

The interaction of hadronic jets with background matter in active galactic nuclei (AGNs) as a possible source of γ-rays has been problematic because of the difficulty of finding a dense enough target. In principle, such a target might be created either by the matter of a thin accretion disk (Nellen, Mannheim, & Biermann 1993) or by the matter in a corona of a thick accretion disk (Bednarek 1993). The γ-ray emission observed from blazars might originate in hadronic collisions of a highly collimated proton beam with clouds entering the jet. This model, recently proposed by Dar & Laor (1997) and Dar (1998), is similar to the scenario investigated by Burbidge (1956) and Felten (1968) and further explored by Rose et al. (1984, 1987).

In the broad-line region (BLR), the typical dimensions of clouds are of order $\sim 10^{12}$–10^{13} cm with cloud densities $\sim 10^{10}$–10^{12} cm^{-3}. These clouds can be anchored in massive stars, and therefore they need not be destroyed immediately by the jet effects. In fact, the jet plasma and radiation can be responsible for the production of a very

[1] E. O. Hulburt Center for Space Research, Naval Research Laboratory, Washington, DC 20375.
[2] Center for Earth Observing and Space Research, Institute for Computational Sciences and Informatics, George Mason University, Fairfax, VA 22030.
[3] St. John's College, Annapolis, MD 21404.
[4] Department of Experimental Physics, University of Łódź, ul. Pomorska 149/153, PL 90-236 Łódź, Poland.

strong stellar wind, which can be identified with the BLR clouds in active galaxies. For the parameters of the clouds mentioned above, the hadronic collisions occur frequently enough to produce the observed fluxes of γ-rays. Interestingly, Dar (1998) has proposed that the source of the BLR clouds is ablated planetary material anchored to stellar systems in the cores of AGNs and that the TeV and γ-ray flares seen in some AGNs are the interaction of residual cometary material with the relativistic jet.

Collisionless processes principally driven by the two-stream instability (Scott et al. 1980; Rose et al. 1984, 1987) can be the dominant energy-loss mechanism for such jets in parameter ranges associated with the BLR and narrow-line region (NLR) (Beall 1990). The computations by Dar & Laor do not take into account these collisionless energy losses as the jet propagates through the dense, hot medium of the cloud.

Where collisionless energy losses are significant, propagation lengths are markedly shortened. This is especially true for electron-proton beams with relatively low Lorentz factors (see Rose et al. 1984; Beall 1990). These effects must be taken into account when calculating the γ-ray emission from the jet.

The radiation emitted by a relativistic electron-proton beam interacting with an ambient medium such as a broad-line cloud has been previously discussed in general terms by Rose et al. (1987) and Beall et al. (1987). In this paper, the predictions of the model wherein an electron-proton beam interacts with an interstellar cloud are compared with the results of γ-ray observations of Mrk 421 in high and low states. We extend the results of the recent discussion of this model by Dar & Laor (1997) to take into account the influence of collisionless losses on the electron-proton jet's γ-ray spectrum.

2. HADRONIC JETS IN ACTIVE GALAXIES

One of our basic assumptions in this model is that collimated, highly relativistic beams of hadrons (with Lorentz factors up to $\sim 10^4$) propagate in the cores of active galaxies. In fact, the existence of plasma motions with Lorentz factors $\gamma \gg 10$ in the inner jets of blazars is suggested by the observations of intraday variability in some sources, which in turn allows one to infer the brightness temperatures $\sim 10^{17}$–10^{21} K, many orders of magnitude higher than the inverse Compton limit (e.g., Begelman, Sikora, & Rees 1994; review by Wagner & Witzel 1995). For example, recently observed brightness temperatures of $\sim 10^{21}$ K in the quasar PKS 0405−385 imply a bulk Lorentz factor for the emission region in the jet of $\gamma \sim 10^3$ (Kedziora-Chudczer et al. 1997; Wagner, von Montigny, & Herter 1997). Additionally, Mukherjee et al. (1997) have presented data from the *CGRO* EGRET that show detections of 51 blazars within an energy band of 0.2–1 GeV.

Indeed, such a scenario is not new. Burbidge (1956) first suggested, based on observations of polarized optical emission in M87, that protons were necessary to transport the energy along the extended length of the jet from its source in the core to the AGN. In that paper, Burbidge discussed the collisional processes that could supply the energetic $e^{\pm}$ pairs thought to be responsible for the optical synchrotron emission. This model was also considered by Felten (1968), who suggested additionally that plasma processes cannot be ruled out as an acceleration mechanism for the optically emitting synchrotron electrons. In fact, our work is kindred to the original paper by Felten (1968), since Felten used the then-available work on plasma instabilities to delimit models for the emitted radiation.

So far it is not clear how such highly collimated beams—which seem to be suggested by γ-ray and TeV-range observations—could be produced in active galaxies, although several intriguing possibilities have been suggested.

The required huge potential drops can appear in the inner part of an accretion disk around a massive black hole as a result of reconnection of magnetic fields magnified by the disk differential rotation (Haswell, Tajima, & Sakai 1992). In this scenario, relativistic electron and proton beams can be produced in regions in which magnetic field line reconnections occur. This mechanism can also operate in the accretion disk corona (Lesch & Pohl 1992) or in the jet (Romanova & Lovelace 1992).

It is plausible that highly relativistic particles can be accelerated by the induction of strong electric fields created by a black hole surrounded by a rotating accretion disk with an embedded perpendicular magnetic field (e.g., Blandford & Znajek 1977; Lovelace 1976; Blandford 1976). In a recent paper, Subramanian, Becker, & Kazanas (1998) have proposed a related mechanism in which proton acceleration arises as a consequence of second-order Fermi acceleration occurring above the accretion disk in a corona threaded by field lines anchored in the disk. The magnetic "kinks" that arise in their scenario are, in effect, scattering centers that produce a second-order Fermi acceleration of the protons in the corona. The asymptotic, bulk Lorentz factor of the protons in their model is $\gamma \sim 3$–10, or of order 3–10 GeV.

Since the magnetic field lines can be directly linked to the accretion disk until very near the black hole event horizon, it is to be expected that the plasma from the accretion disk cannot penetrate into this region without some difficulty. In fact, we suppose that this may bear on the question of particle acceleration in a rather direct way. However, protons from the disk might also be injected into the base of the jet via decay of neutrons produced in the hot inner part of the accretion disk.

Simulations show that the spectrum of particles injected from a single reconnection region can be a power law (e.g., Schopper, Lesch, & Birk 1998; Mori, Sakai, & Zhao 1998). Almost rectilinear acceleration can also occur when the particles drift along the surface of a relativistic oblique shock front (e.g., Begelman & Kirk 1990). Such shocks may form when the relativistic jet plasma meets some obstacle (e.g., a massive object star, a neutron star, or remnants of supernova explosions; e.g., Bednarek & Protheroe 1997b).

Recently, Ostrowski (1998a, 1998b) has proposed that high-energy cosmic rays can be created by the interaction of background-ionized particles with a relativistic jet through multiple reflections of the background particles off of magnetic irregularities at the jet boundary, this via the Fermi mechanism (Fermi 1949). Each time the particle crosses the jet boundary, its energy will be boosted by a factor proportional to the square of the jet Lorentz factor. The spectrum of particles accelerated by this mechanism is that of a relatively flat power law.

Relativistic jets appear to be ubiquitous features, certainly in the literature, and quite likely in the sky.

The collimation of such highly relativistic jets is probably supported by a magnetic field that is predominantly parallel to the jet axis and toroidal around the jet. Such magnetic

field geometries in the inner strong jets are also inferred by the observations of polarization of jet radio emission (e.g., Begelman, Blandford, & Rees 1984; Saikia & Salter 1988).

The relativistic jets produced in such a picture can be decelerated by interactions with the ambient medium in various ways.

3. PROPAGATION OF RELATIVISTIC ELECTRON-PROTON BEAMS THROUGH INTERSTELLAR CLOUDS

Burbidge (1956), Felten (1968), Rose et al. (1987), and Beall et al. (1987) have suggested that hadronic interactions between the jet and the ambient medium in an AGN could produce high-energy γ-rays. Rose et al. (1984, 1987) first calculated in detail the mechanisms of energy loss for a relativistic, low-density beam of electrons, electrons and positrons, or electrons and protons as it interacts with clouds in the BLR and NLR of AGNs. This work has been amplified by a number of authors, including Beall (1990) and Dar & Laor (1997).

As noted previously, the existence of very high brightness temperatures suggests bulk relativistic flows, while the observed collimation of the superluminal jets in AGNs could be supported by a magnetic field that is predominantly parallel to the jet axis and toroidal around the jet. Such magnetic field geometries in the inner core radio jets are inferred from jet polarization studies as Begelman et al. (1984) and Saikia & Salter (1988) note. Beall, Guillory, & Rose (1998) and Rose et al. (1998) have conducted "benchmark" studies of the propagation model discussed below using a fully relativistic, two-dimensional particle-in-cell (PIC) code with a co-linear magnetic field but in a parameter range that is practicable for the PIC code algorithms. The propagation lengths derived with the PIC code are in substantial agreement with the calculations presented here.

We may parameterize the magnetic field intensity B and the Lorentz factor γ of the beam by requiring that the gyroradius of the beam electrons and protons be large compared to the scale of the BLR clouds, or, alternatively, that the gyroradius be large compared to the propagation scale length L_p due to collisionless processes. For the condition that the gyroradius must be large compared to the BLR cloud size, i.e., R_{L_p} and $R_{L_e} \gg L_c$, where L_c is the scale size of the BLR clouds. If we suppose that the jet propagates in a magnetic field essentially collinear with the jet's axis, there is no net effect on the beam propagation direction, a situation that also occurs for $B \sim 0$. For finite B and requiring that $L_c \ll R_{L_e}$ and R_{L_p}, we find that $B \sin\theta \ll 1.7 \times 10^{-8}$ to 1.7×10^{-11} for electrons and $B \sin\theta \ll 3.4 \times 10^{-5}$ to 3.4×10^{-8} for protons for BLR clouds of 10^{11} and 10^{14} cm, respectively. This implies that for electrons with $\gamma = 10^4$ and $\theta = 1°$, $B \ll 1.7 \times 10^{-4}$ to 1.7×10^{-7} G and for $\gamma = 10^2$ and $\theta = 1°$, $B \ll 9.7 \times 10^{-5}$ to 9.7×10^{-8}. The equivalent constraint for protons yields, for $\gamma = 10^4$ and $\theta = 1°$, $B \ll 1.9 \times 10^{1}$ to 1.9×10^{-2} and for $\gamma = 10^2$ and $\theta = 1°$, $B \ll 1.9 \times 10^{-1}$ to 1.9×10^{-4}. It is plausible that the interaction of beam protons and beam electrons will effectively drag the beam electrons to the larger gyroradius of the relativistic protons.

It is perhaps more natural to set constraints on the parameters of the model by requiring that the beam stopping length L_p due to plasma processes be small compared to the gyroradius due to interactions with the ambient magnetic field in the cloud. To do this, we must calculate the energy losses due to collisionless processes and determine the propagation length implied by them.

The presence of a significant, transverse component of the magnetic field will in effect heat the beam and reduce the degree of collimation of the jet. The presence of significant magnetic fields will thus transform the initial growth rate of the two-stream instability from a "cold-beam" to a "warm-beam" mode (see, e.g., Kaplan & Tsytovitch 1973; Rose et al. 1984). Here, we consider only the cold-beam case, principally because of the apparent high level of collimation of jets from blazars, although the possibility of such a transition (from cold to warm beam and from zero beam opening angle to a finite one) might bear on our finding a natural distinction between blazar-type sources and other AGNs. The instabilities discussed here are the principal energy-loss mechanisms for the relativistic jet.

As the beam of relativistic particles deposits energy in the ambient medium via the generation of electrostatic plasma waves, a number of important physical processes are operant. The material in the jet cone or cylinder suffers periodic acceleration as the two-stream instability generates regions of high electric field intensity, which then further "sweep out" electrons (and eventually background atoms) from the region in which the high electric fields are generated. These "cavitons" are low-density, microscopic structures that have a net motion with respect to the ambient medium. During the time during which they form, evolve, and then collapse (much like a wave breaking on a shore), they transfer momentum to the ambient medium in the direction of the jet's motion.

In addition to the transfer of momentum to the ambient medium by the net motion of the electric fields in the cavitons, a high-frequency component of the caviton electric field interacts with electrons in the ambient medium in a manner that evolves the Maxwell-Boltzmann distribution of the gas, producing a high-energy tail. This high-energy tail is a remarkably efficient mechanism for ionizing the gas in the broad- and narrow-line regions of AGNs (Beall & Guillory 1996). In addition, the high-energy tail on the Maxwell-Boltzmann distribution can decrease the growth rate of the parametric (oscillating two-stream) instability (Freund et al. 1980) and thus effects the heating rate of the beam upon the plasma and the cooling rate via inelastic processes and radiation transport.

In order to calculate the propagation length of the electron-proton jet described above, we model the interaction of the relativistic jet with the ambient medium through which it propagates by means of a set of coupled, partial differential equations that describe the growth, saturation, and decay of the three wave modes likely to be produced by the jet–ambient medium interaction. First, two-stream instability produces a plasma wave W_1, called the resonant wave, which grows initially at a rate $\Gamma_1 = (\sqrt{3}/2\gamma)(n_b/2n_p)^{1/3}\omega_p$, where γ is the Lorentz factor of the beam, n_b and n_p are the beam and cloud number densities, respectively, and ω_p is the plasma frequency. Second, a parametric instability fed by this wave generates high-frequency components to the electrostatic waves in the plasma. These high-frequency components we designate as W_2. Finally, the interaction of these waves with one another and with the ions in the ambient medium generate ion-acoustic waves, which we designate as W_s. Such a treatment of the process considered herein does not of course provide a self-consistent calculation of the deposition of the beam

energy into the plasma. It does, however, provide a reasonable estimate of the magnitude of the effects of the interaction of the relativistic jet with the ambient medium. A more detailed discussion of the considerations leading to these rate equations can be found in Scott et al. (1981), Rose et al. (1984, 1987), Beall et al. (1987), and Beall (1990). The results of these estimates have been substantially confirmed by a PIC code simulation (Beall et al. 1998; Rose et al. 1998) in parameter ranges in which PIC code simulations are computationally practicable. The introduction of a weak, longitudinal magnetic field along the beam axis stabilizes the beam against a filamentation instability and increases its propagation length somewhat.

The time-dependent values of the normalized wave energy densities for the two-stream instability W_1, the oscillating two-stream instability W_2, the ion-acoustic waves W_s, and the shortest timescale for the growth of the instabilities τ determine the rate at which energy is drawn from the relativistic beam into the ambient medium. We note that $\tau = 1/\Gamma_1$, where Γ_1 is the initial growth rate of the two-stream instability wave energies. These solutions represent a spatial average of the energy density for the waves in the plasma.

As a beam excites waves in traversing a background plasma, it loses energy and γ decreases. For an electron-proton beam, the principal collisionless interaction is between the beam electrons and background plasma. Consequently, the beam electrons will tend to slow down with respect to the beam protons. If the beam-plasma interaction is not very strong, the beam protons will drag the electrons along with them.

For a relativistic beam, $v_b = c(1 - v^2/c^2)^{-1/2}$ and the energy loss through a distance Δl can be estimated as follows. Let

$$v_b n_b m' c^2 (d\gamma/dx)\Delta \simeq -d(\alpha\epsilon_1)/dt \ , \tag{1}$$

where $m' = m$ for an electron beam, $m' = m$ for an electron-positron beam, $m' = m_p + m$ for an electron-proton beam, ϵ_1 is the energy density of the resonant waves, and α is a factor (≥ 1) that corrects for the simultaneous transfer of resonant wave energy into nonresonant wave energy ϵ_2 and ion-acoustic wave energy ϵ_s. From equation (1), we find

$$dE/dx = -(1/n_b v_b)(d\alpha_1/dt) \tag{2}$$

and

$$\int \gamma = -\int [d(\alpha\epsilon_1)/dt]/(v_b n_b m' c^2) \ . \tag{3}$$

This equation can be compared directly with the equations for the individual (collisional) particle energy-loss mechanisms (Beall 1990). We note that $\alpha\epsilon_1 = \alpha W_1/nkT$ and that dt is the cycle time between periods in the oscillatory solutions to the equations or, for the steady state solutions, roughly $1/\Gamma_1$. The two time intervals are approximately equal.

Given these considerations, the propagation length L_p [i.e., the distance over which $\gamma = (1 - v^2/c^2)^{-1/2}$ decreases by a factor of ~ 2] becomes

$$L_p = (\gamma/2) v_b n_b m' c^2 / \langle d\alpha e_1/dt \rangle \ , \tag{4}$$

where $\langle d\alpha e_1/dt \rangle$, the time-averaged rate of excitation of wave energy density, can be obtained from the time-dependent solutions to the systems of equations described above and in Rose et al. (1984).

Figure 1 shows the dependence of propagation length L_p versus γ_b for a range of parameters appropriate for the BLRs of AGNs.

We can now compare the jet propagation lengths to the gyroradii for various parameters in the clouds. Of course, with no magnetic field, the jet will propagate through the cloud essentially linearly, heated only by collisional and collisionless processes discussed above and in Beall (1990). For a finite magnetic field, we require that $L_p < R_{L_p}$, assuming that the electron-proton interactions in the jet cause the jet electrons to track the protons. Given these constraints, for $\gamma = 10^4$, $B = 10^{-7}$, and $\theta = 1°$, $R_{L_p} = 1.8 \times 10^{19}$ cm for protons, while for $\theta = 10°$, $R_{L_p} = 1.8 \times 10^{18}$ cm. For this value of γ, the collisionless plasma processes produce $L_p \sim 1 \times 10^{15}$–$5 \times 10^{16}$, as n_b ranges from 10^1 to 10^5 cm^{-3} and for a cloud density $n_c = 1 \times 10^{12}$ cm^{-3} and $T = 10^4$ K.

Similarly, for $\gamma = 10^4$, $B = 10^{-5}$ and $\theta = 1°$, $R_{L_p} \sim 1.8 \times 10^{17}$ cm, while for $\theta = 10°$, $R_{L_p} \sim 1.8 \times 10^{16}$ cm. Finally, for $B = 10^{-3}$ and $\theta = 1°$, $R_{L_p} \sim 1.8 \times 10^{15}$ cm for protons, while for $\theta = 10°$, $R_{L_p} \sim 1.8 \times 10^{14}$ cm.

To illustrate the range of possible values, we also take $\gamma = 10^2$ and $B = 10^{-2}$. For $\theta = 1°$, $R_{L_p} = 1.8 \times 10^{12}$, while for $\theta = 10°$, $R_{L_p} = 1.8 \times 10^{11}$ cm. For these parameters, the plasma losses have a range of $L_p = 1 \times 10^{11}$–5×10^{12} cm, as n_b ranges from 10^1 to 10^5 cm^{-3} and for a cloud density $n_c = 1 \times 10^{12}$ cm^{-3} and $T = 10^4$ K.

Finally, for $\gamma = 10^2$, $B = 10^1$, and $\theta = 1°$, $R_{L_p} = 1.8 \times 10^9$, while for $\theta = 10°$, $R_{L_p} = 1.8 \times 10^8$ cm. In this case, the jet and the magnetic field in the ambient medium must be very closely aligned for $L_p \geq R_{L_p}$ for values of $B \geq 10^1$.

Therefore, L_p typically can be shorter than the gyroradius for an equivalent electron-positron or electron-proton beam, and the beam will likely retain a significant degree of collimation over distance that the jet propagates with bulk relativistic motion. This pattern is a characteristic of the nonlinear plasma processes that pull energy from the beam: for higher γ's, the energy loss becomes relatively smaller

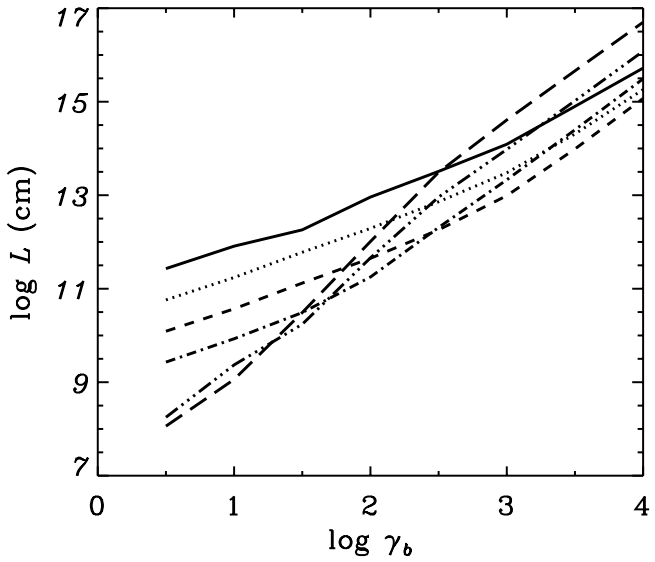

FIG. 1.—Characteristic propagation distances L_p for the electron-proton beam as a function of its Lorentz factor. Specific curves show the results for beam densities $n_b = 1$ (*solid*), 10 (*dotted*), 10^2 (*dashed*), 10^3 (*dot-dashed*), 10^4 (*triple-dot–dashed*), and 10^5 cm^{-3} (*long-dashed*). The results are shown for temperature of the cloud $T = 10^4$ K and its density $n_c = 10^{12}$ cm^{-3}.

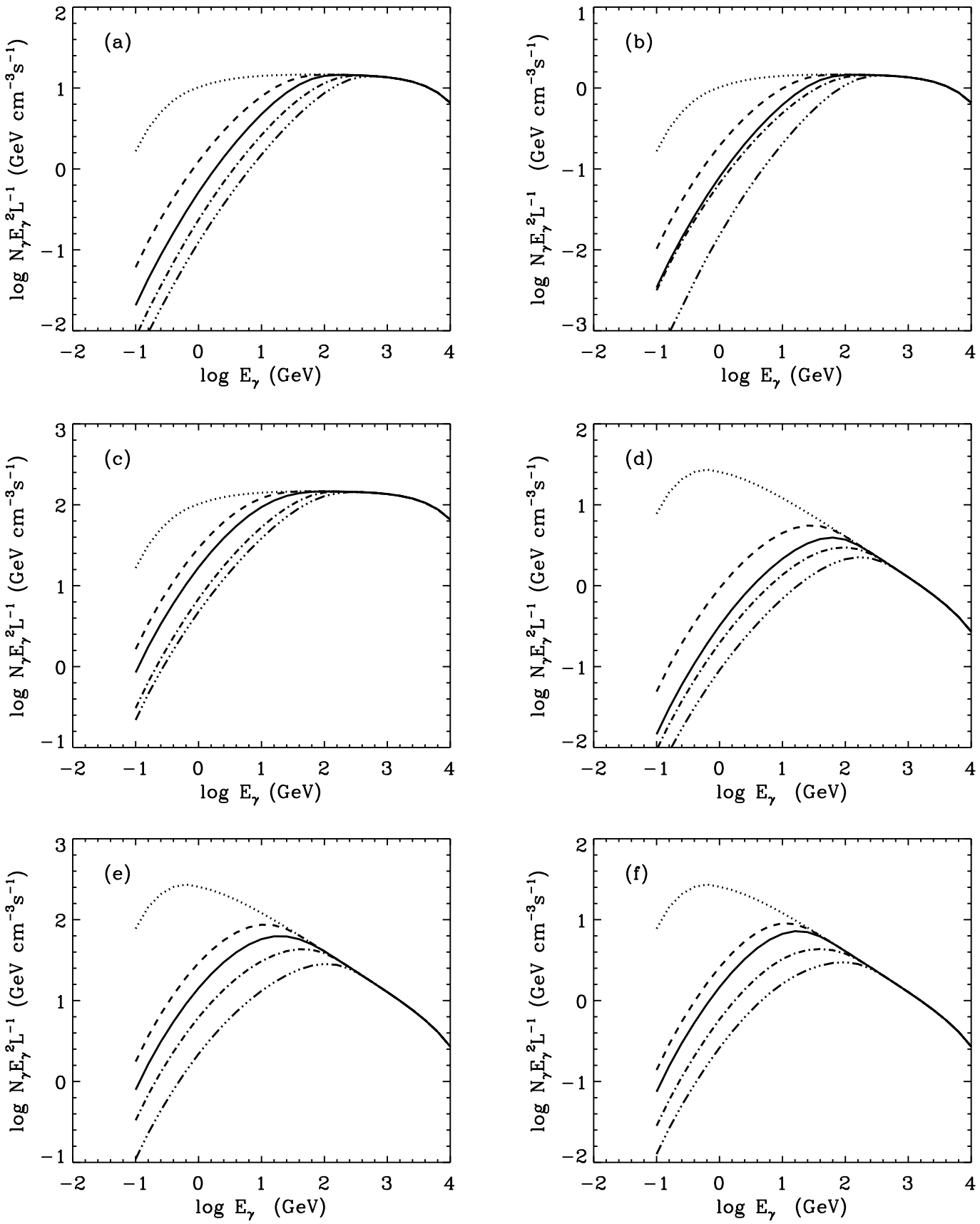

FIG. 2.—(*a*) The γ-ray spectra produced during propagation of relativistic electron-proton beam in the cloud with inclusion of collisionless losses. These results are shown for the power-law spectrum of protons with the spectral index $\alpha = 2$ [see (*a*), (*b*), and (*c*)] and $\alpha = 2.5$ [see (*d*), (*e*), and (*f*)] and normalization (*a*) $A = 10^5$, (*b*) 10^4, and (*c*), (*d*), (*e*), (*f*) 10^6. The proton beam propagates in the cloud with the density (*a*), (*b*), (*d*), (*f*) $n_c = 10^{12}$ cm^{-3} and (*c*), (*e*) $n_c = 10^{13}$ cm^{-3} and temperature (*f*) $T_c = 10^3$ K and $T_c = 10^4$ K in all other panels. The specific curves correspond to different propagation distances in the cloud $L = 10^{12}$ cm (*dashed curve*), 3×10^{12} cm (*full curve*), 10^{13} cm (*dot-dashed curve*), and 3×10^{13} cm, except (*c*) and (*e*), for which the propagation distances are an order of magnitude lower. The dotted curve shows the γ-ray spectrum in the case when collisionless losses are not included.

outside of the region close to the disk where inverse Compton losses are significant.

We believe that these collisionless plasma processes slow the jet in the early stages of its propagation, allowing for a transition from ultrarelativistic to supersonic flow, where hydrodynamic processes dominate.

Estimates of the magnetic field in the ambient medium associated with the jet-cloud interaction vary. Felten (1968), for example, has estimated $B_{\perp} \leq 3 \times 10^{-5}$ G for M87, based on energy transport and lifetime considerations.

We now turn to a calculation of the γ-ray spectra that can be associated with the jet-cloud interactions.

4. GAMMA RAYS FROM INTERACTION OF ELECTRON-PROTON BEAMS WITH DENSE CLOUDS

The electron-proton (*e-p*) beams, propagating through the ambient medium in the core of an active galaxy, suffer energy losses via collisionless excitation of plasma waves (Rose et al. 1984), through hadronic collisions with matter and various other collisional processes (Beall 1990). In hadronic collisions, neutral and charged pions are created. These decay to electrons and positrons, γ-rays, and neutrinos. Electrons and positrons can later lose energy via bremsstrahlung, inverse Compton scattering, and synchrotron processes.

The spectrum of the protons injected from a single reconnection in the region where the jet is accelerated might be nearly monoenergetic, since all particles could then pass through the same electric field potential, or it might resemble a power law if the escape of particles from the reconnection region is stochastic (Colgate 1995). Even if the proton spectrum that emerges from a single reconnection region is monoenergetic, the total spectrum summed up over many reconnection regions is likely to resemble a power law. Therefore, it seems reasonable to consider a power-law spectrum of the proton beam, as Dar & Laor (1997) have done.

We compute the spectra of γ-rays from decay of neutral pions produced in the interaction of such a proton beam with a cloud that enters the jet. During propagation through the cloud, the *e-p* beam Lorentz factor γ_b changes as a result of collisionless energy losses according to

$$\gamma_b(x) = \gamma_{b,0} \times 2^{-x/L_p} , \quad (5)$$

where x is the propagation distance in the cloud and $\gamma_{b,0}$ is the initial Lorentz factor of the *e-p* beam.

The differential γ-ray spectrum from interaction of the *e-p* beam with a single cloud can be obtained from

$$N_{\gamma} \equiv \frac{dN_{\gamma}}{dE_{\gamma}\, dS dt} = \int_0^L \int_{E_{p,\min}}^{E_{p,\max}} \frac{dN_p}{dE_p\, dV} \frac{dN_{\gamma}(E_p)}{dE_{\gamma}\, dt} dE_p\, dx , \quad (6)$$

where $dN_p/dE_p\, dV = AE_p^{-\alpha}$ is the differential density of relativistic protons (per energy and volume) which is assumed to be a power-law type with the index α and normalization A, $dN_{\gamma}(E_p)/dE_{\gamma}\, dt$ is the differential γ-ray photon spectrum produced per unit time by monoenergetic protons with energy $E_p = m_p \gamma_b$, L is the maximum propagation distance in the cloud, and m_p is the proton rest mass. In computations of these spectra, the scaling model has been used (Stephens & Badhwar 1981) which gives a good approximation for the *p-p* cross section in the proton energy range considered.

The computations of the γ-ray spectra have been done for different initial spectra of proton beams defined by α and A. In Figure 2 we show such γ-ray spectra, multiplied by the square of photon energy and divided by the propagation distance L in the cloud, for $\alpha = 2$ (Figs. 2*a*, 2*b*, and 2*c*) and $\alpha = 2.5$ (Figs. 2*d*, 2*e*, and 2*f*) for different normalizations $A = 10^4$, 10^5, and 10^6. Different curves show the γ-ray spectra for different propagation distances of the proton beam in the cloud, and the dotted curve shows the γ-ray spectrum in the absence of collisionless losses. The beam power for the applied proton spectrum is comparable to the expected jet power in AGNs. For example, if the jet radius is $S = 10^{16}$ cm^{-2} and $\alpha = 2$ and $A = 10^5$, then the proton beam power is $P_b = cSA \int_{E_{th}}^{E_{p,\max}} E_p^{-2} E_p\, dE_p \approx 10^{46}$ ergs s^{-1} for $E_{p,\max} = 10^4$ GeV. Since the parameters of the cloud determine the propagation distance of the proton beam, the γ-ray spectra are computed for the cloud densities $n_c = 10^{12}$ and 10^{13} cm^{-3} and temperatures $T_c = 10^4$ and 10^3 K. Such cloud parameters are expected in the broad-line regions of AGNs (Dar & Laor 1997). For the range of investigated parameters, the γ-ray spectra show a characteristic break located between 10 and 100 GeV.

5. CONFRONTATION OF THE PROTON BEAM MODEL WITH OBSERVATIONS OF MARKARIAN 421

Mrk 421 shows strong flares observed simultaneously in the TeV and X-ray energy range on timescales from days up to 15 minutes (e.g., Buckley et al. 1996; Gaidos et al. 1996). The spectrum observed by the Whipple Observatory during a strong flare on 1996 May 7 has the spectral index $2.56 \pm 0.07 \pm 0.1$ between 0.3 and 10 TeV (McEnery et al. 1997). The spectrum of Mrk 421 observed during low TeV state by the EGRET telescope between 100 MeV and a few GeV has the spectral index 1.71 ± 0.15 (Lin et al. 1994). This spectrum does not change significantly between the low and high TeV states (Buckley et al. 1996). Similar flaring behavior is also observed in the case of Mrk 501 in the TeV energy range (see the review by Protheroe et al. 1997) and in X-rays (Catanese et al. 1997; Pian et al. 1998). Below we discuss the expected radiation signatures from the proton-cloud interaction model in the context of these observations.

5.1. *Gamma Rays from Decay of* π^0

The existence of a break in the γ-ray spectra of two BL Lac objects (Mrk 421 and Mrk 501) observed in the TeV energy range is at present very clear. The relativistic proton beam model with a single power-law spectrum is able to explain this feature quite naturally.

In order to find out if the model is able to explain the shape of the γ-ray spectrum observed from Mrk 421 in the TeV and GeV energy range, we compare in Figure 3 the results of observations with the expected emission from the beam-cloud collision model. We assume that the strong variability of the TeV emission is caused by the proton beam propagating through regions of cloud(s) with different thickness L.

The much lower variability of the MeV–GeV γ-ray flux is generally consistent with the expectations of the proton beam model. The computed spectra also show a break between the GeV and TeV energy range, consistent with the observations of Mrk 421 and Mrk 501. This break is caused by the collisionless losses of the *e-p* beam. However, if the computed spectrum is normalized to the spectrum observed in the TeV energies, then the predicted GeV spectrum is significantly flatter, being inconsistent with the spectral

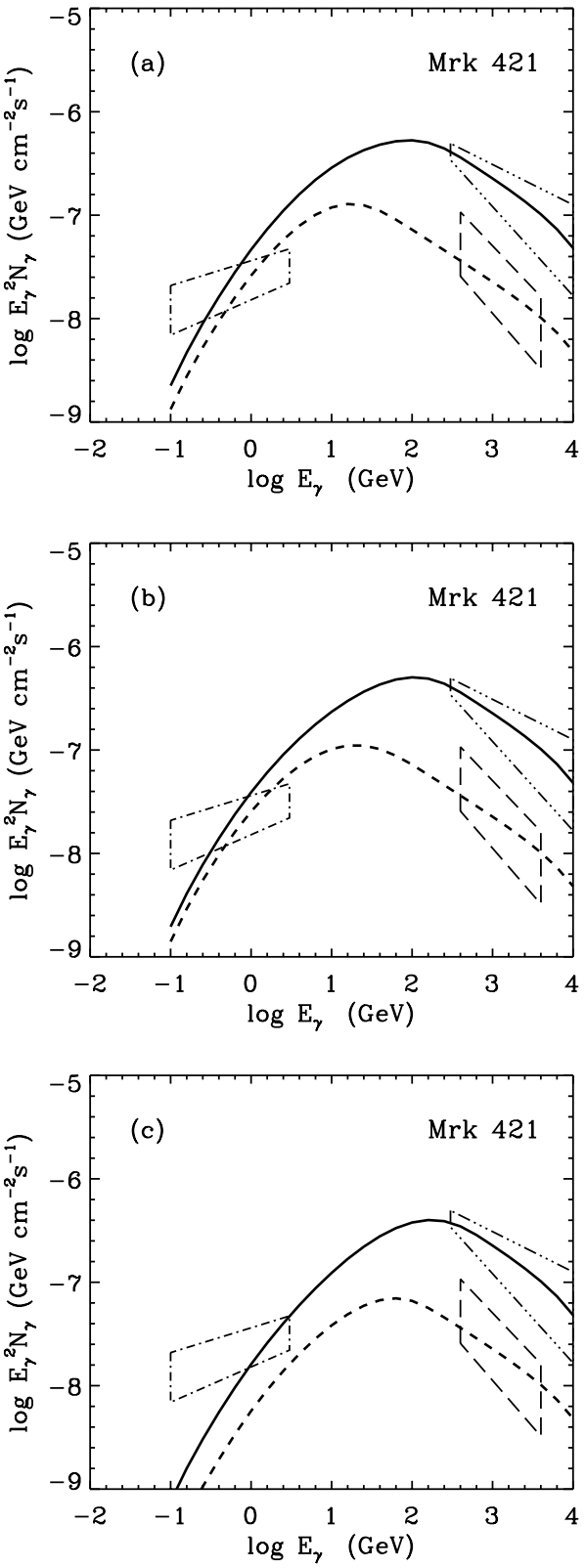

FIG. 3.—Differential γ-ray spectra from decay of neutral pions produced by proton beam with the power-law spectrum and index 2.5 are compared with the observations of Mrk 421 by the EGRET telescope (*dot-dashed box*; Lin et al. 1994), by the Whipple Observatory in a low state (*dashed box*; Mohanty et al. 1993), and in a high state (*triple-dot–dashed box*; McEnery et al. 1997). Two γ-ray spectra correspond to different propagation distances in the cloud equal to $L = 3 \times 10^{13}$ (*solid curve*) and $L = 3 \times 10^{12}$ cm (*dashed curve*) in (*a*) and (*c*) and for an order of magnitude lower propagation distances in (*b*). The parameters of the proton beam and the cloud in (*a*), (*b*), and (*c*) are these same as in Figs. 2*f*, 2*e*, and 2*d*, respectively.

index in the GeV energies observed by EGRET (Lin et al. 1994; Buckley et al. 1996). Therefore, the γ-rays produced from the decay of neutral pions cannot by themselves be used to explain the weakly variable GeV emission observed from Mrk 421 unless the spectrum of protons in the beam show strong steepening below $\sim$10 GeV. Contributions from another source of γ-rays to the GeV energy range is needed at least at energies below $\sim$1 GeV. In the next subsection, we discuss contributions to the emitted radiation from secondary $e^\pm$ pairs.

5.2. *Photons Produced by Secondary $e^\pm$ Pairs from the Decay of $\pi^\pm$*

If the jet-cloud model is valid for the γ-ray production in Mrk 421, then the secondary $e^\pm$ pairs from the decay of charged pions should have a spectrum very similar to the γ-ray spectrum from π^0 decay but shifted to lower energies by a factor of 2. Let us assume, following Dar & Laor (1997), that these secondary $e^\pm$ pairs are responsible for the production of synchrotron emission during the outburst in Mrk 421. In fact, the equilibrium spectra of secondary $e^\pm$ pairs are consistent with the synchrotron spectrum observed from Mrk 421 in a high state. The break in the spectrum of secondary pairs at $E_{e^\pm,b}$ should correspond to the break in the synchrotron spectrum that is observed in Mrk 421 at $\sim$1.65 keV (Takahashi et al. 1996). The relation between these breaks allows us to estimate the strength of the magnetic field in the region of production of synchrotron photons from

$$B \approx 2B_{\rm cr}\,\epsilon_b\, m_e\, E_{e^\pm,b}^{-2}\,, \tag{7}$$

where $B_{\rm cr} = 4.414 \times 10^{13}$ G, and m_e is the electron rest mass. For the value $E_{e^\pm,b} \sim 100$ GeV (see Fig. 3), the magnetic field in the emitting region should be equal to $B \approx 7.1$ G. The characteristic cooling time of secondary pairs with energies mentioned above in such a magnetic field is of the order of $\sim$70 s, which is consistent with the timescale of outbursts in Mrk 421.

The X-ray and γ-ray flares have similar powers in Mrk 421. Therefore, the secondary pairs must move almost ballistically through the cloud, e.g., by following highly ordered magnetic field lines along the jet axis. The pairs move through the dense cloud during the characteristic time $t_c \approx r_c/c$, which is comparable to their characteristic synchrotron cooling time estimated below. Therefore, the observed synchrotron emission is produced close to the cloud and should be synchronized with the TeV γ-ray emission.

The comparison of synchrotron and bremsstrahlung cooling times of secondary $e^\pm$ pairs shows that bremsstrahlung dominates for $e^\pm$ pairs with Lorentz factors

$$\gamma < \gamma_{\rm bs} \approx 4.4 \times 10^{-7} n_{\rm H} B^{-2}\,, \tag{8}$$

where $n_{\rm H}$ is the density of the background matter. For the value of the magnetic field estimated above and considered cloud density $n_{\rm H} = 10^{12}$ cm^{-3}, we get $\gamma_{\rm bs} \approx 9 \times 10^4$. However, the pairs travel through the cloud during the time t_c, which is shorter than their cooling time via bremsstrahlung: $\tau_b \approx 1.4 \times 10^{15} n_{\rm H}^{-1}$ s. Hence, we conclude that secondary $e^\pm$ pairs, with Lorentz factors $\gamma < \gamma_{\rm bs}$, have no time to cool by a bremsstrahlung process in the cloud. This process cannot, therefore, contribute essentially to the Mrk 421 spectrum in the MeV–GeV energy range.

The contribution to the γ-ray spectrum from inverse Compton scattering (ICS) of soft photons by secondary

pairs is very uncertain because of the lack of precise information on the soft photon geometry and density in the emission region. The observations of Mrk 421 by the EGRET and *ASCA* telescopes allow us to estimate the ratio of the power emitted in MeV–GeV γ-rays and X-rays, which is close to 0.5 (see von Montigny et al. 1995; Takahashi et al. 1996). Therefore, if ICS of secondary pairs contributes significantly to the EGRET energy range, the energy densities of the magnetic field and the low-energy radiation in the region of the propagation of the secondary pairs has to be in a similar ratio, provided that the scattering occurs in the Thomson regime. The energy density of the magnetic field in the emission region of Mrk 421 (see above) requires that the energy density of soft photons should be $\rho_{\rm ph} \approx 8 \times 10^{11}$ eV cm^{-3}.

Three different sources of soft photons can provide, in principle, a target for these secondary pairs, i.e., soft synchrotron photons, thermal photons coming directly from an accretion disk, or thermal bremsstrahlung photons produced in the cloud. The two first possibilities can be excluded based on the following arguments. Let us assume that the stable flux of γ-rays in the 100 MeV–1 GeV energy range is produced by ICS in the Thomson regime. The scattering in the Klein-Nishina regime reduces the efficiency of the process and produces too steep a spectrum. The part of the spectrum of secondary pairs below $\sim$10 GeV does not vary strongly (see Fig. 3). However, these pairs can produce 100 MeV–1 GeV γ-rays by scattering synchrotron X-ray photons, which are highly variable. Therefore, the flux of γ-rays in the EGRET energy range should vary significantly between the low and high TeV state, which is in contradiction with the observations (Lin et al. 1994; Buckley et al. 1996). The flux of secondary pairs with energies above $\sim$10 GeV is highly variable and cannot produce EGRET γ-rays by scattering weakly variable optical-UV photons of synchrotron origin or produced in the low-temperature optically thick accretion disk.

The density of thermal bremsstrahlung photons produced in the cloud can be estimated from

$$\rho_{\rm br} \approx 3 \times 10^{-26} T_c^{0.5} n_c^2 r_c \text{ eV cm}^{-3} . \quad (9)$$

However, these photons have characteristic energies $\epsilon_{\rm br} \sim 1$ eV. Hence, they require electrons with Lorentz factors $\sim 3 \times 10^4$ in order to produce 1 GeV γ-rays via an ICS process. Secondary pairs with these energies show already a high level of variability between low and high states of Mrk 421 and therefore should produce strongly variable GeV emission, which is contrary to observations.

The only possibility left is that the secondary pairs with energies below $\sim$10 GeV scatter nonvariable radiation with characteristic energies of $\epsilon_{\rm X} = 0.1$–1 keV of another origin (e.g., produced in the high-temperature disk or the disk corona). However, this radiation field has to be transparent to the observed γ-rays. The optical depth for the GeV γ-rays is less than 1 if the characteristic dimension of this X-ray region is

$$r_{\rm X} < \frac{\epsilon_{\rm X}}{\rho_{\rm ph} \sigma_{\gamma\gamma}} \approx 5 \times 10^{15} \text{ cm} , \quad (10)$$

where $\sigma_{\gamma\gamma}$ is the maximum value of the photon-photon pair production cross section and applying $\epsilon_{\rm X} = 1$ keV. This radiation might eventually originate in the inner part of the accretion disk or the disk corona or might be produced by the low-density but high-temperature plasma surrounding small and dense clouds, which are considered here as a target for relativistic proton beam. However, the above constraint on the dimension of this region rather excludes the last possibility.

6. CONCLUSIONS

If the relativistic electron-proton beam collides with a dense, compact cloud, the energy losses of the jet via the excitation of plasma waves (Rose et al. 1984) become important for beams with energies below $\sim$300 GeV (Fig. 1). This process causes the break in the spectrum of γ-rays from the decay of neutral pions that are produced in inelastic collisions of protons with matter. Such a model can naturally explain the low and high states of TeV γ-ray emission in BL Lac–type blazars, provided that the proton beam interacts with different column densities of matter. Moreover, because of the collisionless energy losses of the proton beam, the γ-ray spectrum predicted in the 100 MeV–1 GeV energy range does not vary strongly. This feature fits nicely with the general behavior of the γ-ray emission from Mrk 421 between low and high states. However, the γ-ray spectra computed in the 100 MeV–1 GeV energy range for reasonable sets of model parameters are too flat, showing significant deficiency in comparison to the Mrk 421 spectrum observed by EGRET (Fig. 3) provided that the spectrum of relativistic protons in the beam is well described by a single power law. Secondary $e^{\pm}$ pairs are also produced in hadronic collisions through decay of charged pions, with the spectra similar to the γ-ray spectra but shifted to lower energies. The higher energy, variable part of the spectrum of secondary pairs (with energies above $\sim$10 GeV) can be responsible for the simultaneous X-ray flares.

Such a picture could work provided that the clouds are not too hot. Otherwise, the TeV γ-rays are absorbed by the thermal bremsstrahlung photons produced in the cloud (see computations of the γ-ray mean free paths on Fig. 3 in Beall et al. 1987). The clouds also cannot be too dense. By reversing equation (5-3), we see that if the cloud density is

$$n_c > 3 \times 10^{25} \rho_{\rm ph} T_c^{-0.5} \lambda^{-1} , \quad (11)$$

where $\lambda = n_c r_c$ is the column density of matter traversed by the proton beam in the cloud, then the secondary electrons are not able to lose energy efficiently by the synchrotron process because of the dominant role of ICS losses on thermal bremsstrahlung radiation produced in the cloud.

The relation of the break in the spectrum of secondary pairs to the break in the X-ray spectrum observed in Mrk 421 allows a derivation of the strength of the magnetic field in the emission region equal to $\sim$7.1 G (eq. [3]). These pairs cannot contribute to the EGRET energy range by production of γ-rays in a bremsstrahlung process or by inverse-Compton scattering of soft photons of synchrotron origin, or coming from the optically thick, low-temperature accretion disk, or bremsstrahlung photons produced in the cloud. Only the scattering of nonvariable, soft X-ray photons (0.1–1 keV) by secondary pairs with energies below $\sim$10 GeV could explain the nonvariable γ-ray emission from Mrk 421 in the EGRET energy range. These photons could be produced in the inner part of the accretion disk.

This research was partially supported by a grant from NASA administered by the American Astronomical Society.

J. H. B. gratefully acknowledges the assistance of a grant from the Newstead Foundation, which was instrumental in the completion of this research, and thanks J. Guillory and D. V. Rose for helpful conversations.

W. B. would like to thank the Institute for Computational Sciences and Informatics at George Mason University (Fairfax, VA) for hospitality during his visit. The work of W. B. is supported by the Komitet Badań Naukowych through grant 2P03D00114.

We also gratefully acknowledge the helpful suggestions of an anonymous referee.

We dedicate this work to S. Karakula (December 1935–July 1996), colleague and friend.

REFERENCES

Aharonian, F., et al. 1997, A&A, 327, L5
Beall, J. H. 1990, Physical Processes in Hot Cosmic Plasmas (Dordrecht: Kluwer), 341
Beall, J. H., Bednarek, W., Karakuła, S., & Tkaczyk, W. 1987, in 20th Int. Cosmic-Ray Conf. (Moscow), 1, 191
Beall, J. H., & Guillory, J. 1996, Mem. Soc. Aston. Italiana, 67, 505
Beall, J. H., Guillory, J., & Rose, D. V. 1998, Observational Signatures of Jet-Cloud Interactions, Proc. Vulcano Workshop May 1997, ed. F. Giovannelli & L. Sabau-Graziati (Bologna: Italian Physical Society), in press
Bednarek, W. 1993, ApJ, 402, L29
———. 1998, Mem. Soc. Astron. Italiana, in press
Bednarek, W., & Protheroe, R. J. 1997a, MNRAS, 287, L9
———. 1997b, in Proc. 25th Int. Cosmic-Ray Conf. (Durban), 3, 313
Begelman, M. C., Blandford, R. D., & Rees, J. 1984, Rev. Mod. Phys., 56, 255
Begelman, M. C., & Kirk, J. G. 1990, ApJ, 353, 66
Begelman, M. C., Sikora, M., & Rees, M. J. 1994, ApJ, 429, L57
Blandford, R. D. 1976, MNRAS, 176, 465
Blandford, R. D., & Znajek, R. 1977, MNRAS, 179, 433
Buckley, J. H., et al. 1996, ApJ, 472, L9
Burbidge, G. R. 1956, 124, 416
Catanese, M., et al. 1997, ApJ, 487, L143
———. 1998, ApJ, submitted
Colgate, S. A. 1995, in Proc. 24th Int. Cosmic-Ray Conf. (Rome), 3, 341
Coppi, P. S., Kartje, J. F., & Königl, A. 1993, in AIP Conf. Proc 280, Proc. *Compton GRO* Symp., ed. M. Friedlander, N. Gehrels, & D. J. Macomb (New York: AIP), 559
Dar, A. 1998, MNRAS, in press
Dar, A., & Laor, A. 1997, ApJ, 478, L5
Dermer, C. D., & Gehrels, N. 1995, ApJ, 447, 103 (erratum 456, 412 [1996])
Dermer, C. D., & Schlickeiser, R. 1992, Science, 257, 1642
Felten, J. E. 1968, ApJ, 1551, 861
Fermi, E. 1949, Phys. Rev., 75, 1169
Freund, H. P., Haber, I., Palmadesso, P., & Papadopoulos, K. 1980, Phys. Fluids, 23, 518
Gaidos, J. A., et al. 1996, Nature, 383, 319
Haswell, C. A., Tajima, T., & Sakai, J.-I. 1992, ApJ, 401, 495
Henri, G., Pelletier, G., & Roland, J. 1993, ApJ, 404, L41
Kaplan, S. A., & Tsytovich, V. N. 1973, Plasma Astrophysics (Oxford: Pergamon), 70
Kedziora-Chudczer, L., et al. 1997, ApJ, 490, L9
Krennrich, F., et al. 1997, ApJ, 481, 758
Lesch, H., & Pohl, M. 1992, A&A, 254, 29
Lin, Y. C., et al. 1994, in AIP Conf. Proc. 304, Proc. Second Compton Symp., ed. C. E. Fichtel, N. Gehrels, & J. P. Norris (New York: AIP), 582
Lovelace, R. V. E. 1976, Nature, 262, 649
Mannheim, K., & Biermann, P. L. 1992, A&A, 253, L21
Mattox, J. R., et al. 1997, ApJ, 472, 692
Mayer, H., & Westerhoff, S. 1996, in Proc. Heidelberg Workshop on Gamma-Ray Emitting AGN, ed. J. G. Kirk (MPI H-V37, 1996; Heidelberg: MPI), 38
McEnery, J. E., et al. 1997, in Proc. 25th Int. Cosmic-Ray Conf. (Durban), 3, 257
McNaron-Brawn, K., et al. 1995, ApJ, 451, 575
Mohanty, G., et al. 1993, in Proc. 24th Int. Cosmic-Ray Conf. (Calgary), 1, 440
Mori, K., Sakai, J., & Zhao, J. 1998, ApJ, 493, 175
Mukherjee, R., et al. 1997, ApJ, 490, 116
Nellen, L., Mannheim, K., & Biermann, P. L. 1993, Phys. Rev. D., 47, 5270
Ostrowski, M. 1998a, MNRAS, in press
———. 1998b, A&AS, submitted
Pian, E., et al. 1998, ApJ, 492, L17
Pohl, M., Hartman, R. C., Jones, B. B., & Sreekumar, P. 1997, A&A, 326, 51
Protheroe, R. J. 1998, in Proc. Towards the Millennium in Astrophysics: Problems and Prospects, ed. M. M. Shapiro & J. P. Wefel (Erice 1996; Singapore: World Scientific), in press
Protheroe, R. J., et al. 1997, in Proc. 25th ICRC (Durban), Highlight Session, in press
Punch, M., et al. 1992, Nature, 358, 477
Quinn, J., et al. 1996, ApJ, 456, L83
Romanova, M. M., & Lovelace, R. V. E. 1992, A&A, 262, 26
Rose, D. V., Beall, J. H., & Guillory, J. 1998, in preparation
Rose, W. K., Beall, J. H., Guilory, J., & Kainer, S. 1987, ApJ, 314, 95
Rose, W. K., Guilory, J., Beall, J. H., & Kainer, S. 1984, ApJ, 280, 550
Saikia, D. J., & Salter, C. J. 1988, ARA&A, 26, 93
Schlickeiser, R. 1996, A&A, 120, 481
Schönfelder, V., et al. 1996, A&AS, 120, 13
Schopper, R., Lesch, H., & Birk, G. T. 1998, A&A, in press
Scott, J. S., Holman, G. D., Ionson, J. A., & Papadopoulos, K. 1980, ApJ, 239, 769
Sikora, M. 1994, ApJS, 90, 923
Sikora, M., Kirk, J. G., Begelman, M. C., & Schneider, P. 1987, ApJ, 320, L81
Stephens, S. A., & Badhwar, G. D. 1981, Ap&SS, 76, 213
Subramanian, P., Becker, P. A., & Kazanas, D. 1998, ApJ, submitted
Takahashi, T., et al. 1996, ApJ, 470, L89
von Montigny, C., et al. 1995, ApJ, 440, 525
Wagner, S. J., von Montigny, C., & Herter, M. 1997, in AIP Conf. Proc. 410, Proc. Fourth Compton Symposium, ed. C. Dermer, M. S. Strickman, & N. J. Kurfess (New York: AIP)
Wagner, S. J., & Witzel, A. 1995, ARA&A, 33, 163
Xie, G. Z., Liu, B. F., & Wang, J. C. 1995, ApJ, 454, 50